Heat transfer from a cylindrical fin in combined free-forced flow

K. Velusamy
Indira Gandhi Centre for Atomic Research, Kalpakkam 603102, India

Vijay K. Garg*
Department of Mechanical Engineering, The Ohio State University, Columbus, Ohio 43210, USA

Received 30 November 1986 and accepted for publication 3 August 1987

Following a simultaneous solution to the conduction problem for the fin and the laminar boundary layer equations for the flowing fluid, heat transfer characteristics for a cylindrical fin washed by a combined forced and free convective flow have been determined when the buoyancy assists as well as when it opposes the main flow. Results are presented for the buoyancy influence parameter in the range $-0.3 \leqslant \Omega \leqslant 5$, dimensionless radius of the fin in the range $1 \leqslant R_0 \leqslant 4$, and the conduction-convection parameter in the range $0 \leqslant N_{cc} \leqslant 6$ along with results of the conventional fin model. It has been found that the conventional model overpredicts the fin effectiveness at small N_{cc} values and underpredicts the same for large N_{cc} values, though the deviation is small. However, the local predictions of temperature distribution and of heat flux by the conventional model are in substantial error.

Keywords: fin heat transfer; free and forced flow

Introduction

Heat transfer from a fin results from a combination of conduction within the fin and convection to the fluid surrounding the fin. The boundary conditions at the interface between the fin and the fluid require continuity in temperature and heat flux. Thus the conductive and convective heat transfers are coupled. Conventionally, however, the fin heat conduction equation alone is solved using a uniform value (taken from the literature) of the heat transfer coefficient. This approach, hereafter called the simple model, leads to wrong results because the heat transfer coefficient generally varies over the fin surface. Although the fin heat conduction equation can be solved numerically for an arbitrarily varying heat transfer coefficient, the problem is that the correct distribution of this heat transfer coefficient is unknown a priori. The only way out, hereafter called the complete model, is to solve the coupled conductive-convective heat transfer problem. Moreover, buoyancy force may also be important. In that case the flow field will also depend on the temperature field.

For rectangular fins, complete model studies have been carried out by Sparrow and Chyu[1] for forced convection, by Sparrow and Acharya[2] for natural convection, and by Sunden[3,4] for mixed convection, only for the case of buoyancy assisting the main flow. Garg and Velusamy[5] reported a simple method based on a similar solution approach for a wide range of Prandtl numbers. The effect of the Prandtl number has also been studied by Sunden[6].

It is well established that the convective boundary layer over a cylinder is thicker than that over a flat plate, owing to the curvature of the cylinder. Hence the results for rectangular fins cannot be applied to cylindrical fins without considerable error. Moreover, for cylindrical fins there exists no similar solution, owing to the curvature terms in the equations. Employing a pseudosimilarity variable and a finite difference method similar to the one described in Ref. 7, cylindrical fins have been considered by Huang and Chen[8] for forced convection and by Huang *et al.*[9] for natural convection. However, the case of mixed convection for cylindrical fins has not been considered before. Moreover, the analysis of Huang and Chen[8] has some deficiencies. For example, for an isothermal fin ($N_{cc}=0$), the nondimensional fin temperature (Ref. 8, Equation 16) is unity. Hence the dimensionless heat transfer coefficient (Ref. 8, Equation 20) and the dimensionless heat flux (Ref. 8, Equation 26) are exactly the same. But the results (Ref. 8, Figs. 2, 3) do not reveal this for the parameter $\lambda=3$. The deviation is about 30%. Moreover, at the base of the fin the heat transfer coefficient and the heat flux must be the same (for all N_{cc} values) because the fin temperature is unity at that point according to the boundary condition. This aspect is not revealed in Ref. 8, at least for $\lambda=3$.

Here we solve for the combined free and forced convection over a cylindrical fin in order to study the effect of various parameters on the local heat transfer characteristics. This is essential for accurate heat transfer calculations. Although the fin conduction equation has been solved by either a relaxation procedure[3,4] or a direct matrix inverse method[8,9], we use the simple Runge-Kutta method of integration[5] without any iteration. Our method is very inexpensive compared to the relaxation method or the matrix inverse method. Results are presented for the effect of various parameters on mixed convection over a cylindrical fin when the buoyancy assists and when it opposes the main flow. These results are also compared with those for the simple model.

Analysis

Consider a laminar free stream with velocity u_∞, temperature T_∞, conductivity K, kinematic viscosity ν, coefficient of volumetric expansion β, and thermal diffusivity α approaching a cylindrical thin fin which is aligned parallel to the oncoming flow (see inset of Figure 1). The fin of radius r_0, length L ($\gg r_0$), and conductivity K_f is attached to a base held at temperature T_0

* On sabbatical leave from Indian Institute of Technology, Kanpur, India; author for correspondence

such that it faces either vertically upward (buoyancy opposing the main flow) or vertically downward (buoyancy assisting the main flow). The flow takes place in a gravitational field of acceleration g and is from the tip ($x=0$) to the base ($x=L$) of the fin. The temperature of the fin is $T_f(x)$, the temperature of the fluid within the boundary layer is $T(x, r)$, and the heat transfer coefficient is $h(x)$.

Defining the dimensionless variables $U=u/u_\infty$, $X=x/L$, $V=v\mathrm{Re}^{1/2}/u_\infty$, $R=r\mathrm{Re}^{1/2}/L$, $R_0=r_0\mathrm{Re}^{1/2}/L$, $\theta=(T-T_\infty)/(T_0-T_\infty)$, $\theta_f=(T_f-T_\infty)/(T_0-T_\infty)$, $\mathrm{Re}=u_\infty L/\nu$, $\mathrm{Pr}=\nu/\alpha$, and $\mathrm{Gr}=g\beta(T_0-T_\infty)L^3/\nu^2$, we obtain the one-dimensional fin conduction equation[10] with negligible tip leakage

$$\frac{d^2\theta_f}{dX^2}=N_{cc}h_N(X)\theta_f \tag{1}$$

with boundary conditions

$$\theta_f(X=1)=1 \qquad \text{and} \qquad \frac{d\theta_f}{dX}(X=0)=0 \tag{2}$$

The boundary layer equations for the laminar, uniform property, viscous flow are

$$\frac{\partial(RU)}{\partial X}+\frac{\partial(RV)}{\partial R}=0 \tag{3}$$

$$U\frac{\partial U}{\partial X}+V\frac{\partial U}{\partial R}=\Omega\theta+\frac{1}{R}\frac{\partial}{\partial R}\left(R\frac{\partial U}{\partial R}\right) \tag{4}$$

and

$$U\frac{\partial\theta}{\partial X}+V\frac{\partial\theta}{\partial R}=\frac{1}{\mathrm{Pr}}\frac{1}{R}\frac{\partial}{\partial R}\left(R\frac{\partial\theta}{\partial R}\right) \tag{5}$$

with the boundary conditions

$U=0=V, \quad \theta=\theta_f(X) \qquad$ at $R=R_0$

$U\to 1, \quad \theta\to 0 \qquad$ as $R\to\infty$

and

$U=1, \quad \theta=0 \qquad$ at $X=0, R>R_0$

where $\Omega=\mathrm{Gr}/\mathrm{Re}^2$; the conduction-convection parameter, $N_{cc}=(2KL/K_fr_0)\mathrm{Re}^{1/2}$, is the ratio of conductive resistance to convective resistance; the dimensionless heat transfer coefficient $h_N(X)=(h(X)L/K)\mathrm{Re}^{-1/2}$ and u and v are the velocity components along the axial and radial coordinates x and r, respectively.

In deriving Equations 3 and 4, we have used Boussinesq approximation to approximate the fluid as incompressible except for the buoyancy term in the momentum equation (Equation 4). The heat transfer coefficient $h_N(X)$ to be used in the conduction equation is an outcome of the solution of the boundary layer equations, but the thermal boundary condition to the boundary layer equations is an outcome of the solution of the conduction equation. The coupling between the conduction and boundary layer equations is expressed by the requirement that the heat flux and the temperature be continuous at the fin-fluid interface. Hence the coupling is provided by

$$h(x)(T_f(x)-T_\infty)=-K\left.\frac{\partial T}{\partial r}\right|_{r=r_0} \tag{6}$$

Solution

The boundary layer equations (Equations 3–5) are solved by a finite difference marching technique, which is a modified form of the one described in Ref. 11 for flow in a circular tube. Retaining the nonlinearity of the inertia terms in Equation 4 and the coupling between Equations 4 and 5, we solve the finite difference equations iteratively by the Thomas algorithm at each marching X-location.

For the solution of the second-order linear ordinary differential equation (Equation 1), two independent solutions θ_{f1} and θ_{f2} are assumed such that

$$\theta_{f1}(X=1)=1, \qquad \frac{d\theta_{f1}(X=1)}{dX}=0 \tag{7}$$

and

$$\theta_{f2}(X=1)=0, \qquad \frac{d\theta_{f2}(X=1)}{dX}=1 \tag{8}$$

Equation 1 is integrated twice from $X=1$ to $X=0$, first with initial conditions 7 and then with initial conditions 8, using the

Notation

C_f	Skin friction coefficient
g	Acceleration due to gravity
Gr	Grashof number
h	Heat transfer coefficient
K, K_f	Thermal conductivity of fluid and fin, respectively
L	Length of fin
N_{cc}	Conduction-convection parameter
Pr	Prandtl number
q	Local heat flux
Q	Overall heat transfer rate
r, R	Dimensional and dimensionless radial coordinate, respectively
r_0, R_0	Dimensional and dimensionless fin radius, respectively
Re	Reynolds number
T, T_f	Temperature of fluid and fin, respectively
u, U	Dimensional and dimensionless axial velocity, respectively
v, V	Dimensional and dimensionless radial velocity, respectively
x, X	Dimensional and dimensionless axial coordinate, respectively
α	Thermal diffusivity of fluid
β	Coefficient of volumetric expansion
$\Delta X, \Delta R$	Grid sizes in axial and radial directions, respectively
ν	Kinematic viscosity of fluid
Ω	Buoyancy influence parameter ($=\mathrm{Gr}/\mathrm{Re}^2$)
ϕ	Fin effectiveness based on an isothermal fin
ρ	Density of fluid
τ	Shear stress on fin surface
θ, θ_f	Dimensionless temperature of fluid and fin, respectively

Subscripts

0	Temperature at base of fin
N	Dimensionless value
∞	Free-stream value
$\bar{}$	Indicates average value

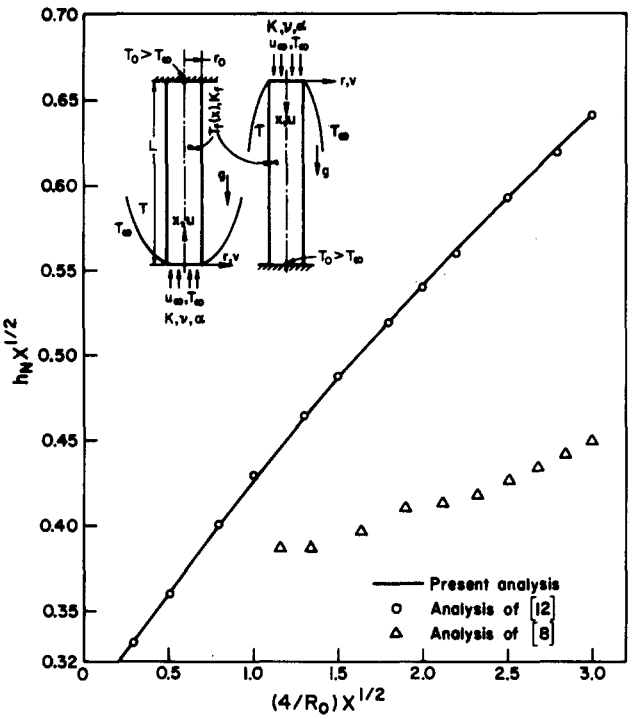

Figure 1 Local heat transfer coefficient for an isothermal cylinder (Pr=0.7, $R_0=\frac{4}{3}$, $\Omega=0$)

fourth-order Runge-Kutta method yielding $\theta_{f1}(X)$ and $\theta_{f2}(X)$. Then the general solution of Equation 1 is a linear combination of $\theta_{f1}(X)$ and $\theta_{f2}(X)$ such that

$$\theta_f(X)=a\theta_{f1}(X)+b\theta_{f2}(X) \tag{9}$$

where the arbitrary constants a and b are determined from the boundary conditions in Equation 2.

The following iterative procedure is followed for the solution of Equations 1–6.

1. A uniform fin temperature distribution such as $\theta_f(X)=1$ is assumed to initialize the iteration process.
2. Using this $\theta_f(X)$ as the boundary condition, we solve the boundary layer equations (Equations 3–5) and calculate the local heat transfer coefficient $h(x)$ using Equation 6.
3. With this $h(x)$, the fin conduction equation (Equation 1) is solved to get $\theta_f(X)$.
4. Steps 2 and 3 are repeated until convergence occurs.

Computational details

Following a step-size study, the step-size in the marching direction (ΔX) was taken as 5×10^{-5} near the tip of the fin ($X=0$) and gradually increased with X up to $X=\frac{1}{2}$. Beyond $X=\frac{1}{2}$, ΔX was gradually decreased to $X=1$ to take care of steeper fin temperature gradients. Along the cross-stream direction very fine grids (of size $\Delta R=0.04$) were concentrated near the fin surface, and comparatively coarser grids ($\Delta R=0.1$) were imposed in the region far away from the fin surface.

For the convergence of the solution the difference in fin temperature values between two consecutive iterations was kept such that

$$[\theta_f^{l+1}(X)-\theta_f^l(X)]/\theta_f^{l+1}(X)\leqslant\varepsilon_1 \qquad \text{for } 0\leqslant X\leqslant 1$$

where l represents the iteration index and ε_1 was taken as 10^{-6} for the results presented here. For the convergence of the boundary layer equations the difference in the velocity distributions between two consecutive iterations was kept such that

$$[U^{l+1}(R)-U^l(R)]/U^{l+1}(R)\leqslant\varepsilon_2 \qquad \text{for } R_0\leqslant R\leqslant R_\infty$$

where R_∞ is the radius of the outer edge of the axisymmetric boundary layer and ε_2 was kept at 10^{-3}. We found almost no change in our results when ε_2 was taken as 10^{-6}, except for the additional computing time. A maximum of eight iterations was required for the conduction equation for the largest N_∞ value. We may also mention that no relaxation was necessary.

Accuracy

For checking our numerical scheme we compared our results for an isothermal fin ($N_\infty=0$) of radius $R_0=\frac{4}{3}$ in pure forced convective flow ($\Omega=0$) with the local nonsimilarity solution of Yu and Sparrow[12] for an isothermal cylinder. Figure 1 shows this comparison for the local heat transfer coefficient. It also displays the erroneous results of Ref. 8. We compared our mixed convection results for isothermal fins of radii $1\leqslant R_0\leqslant 4$ with the local nonsimilarity solutions obtained by Chen and Mucoglu[13] for isothermal cylinders in buoyancy-assisted mixed convective flow. Excellent agreement was obtained.

We also compared the overall fin heat transfer rate Q_N with the heat flux integrated over the convecting fin surface. The deviation was less than 0.6% for all ranges of the parameters considered. In order to test the method by which we solve the conduction equation, we fed a uniform value of heat transfer coefficient to it and compared its results with the analytical solution obtained from the simple model. The results matched exactly.

It can be easily shown that for an isothermal fin, $Q_N=2\pi\bar{h}_N$, where $\bar{h}_N$ is the average heat transfer coefficient for an isothermal fin. Values of $\bar{h}_N$ are given in Table 1.

Results and discussion

For air as the fluid (Pr=0.7), R_0 ranging from 1 to 4, N_∞ ranging from 0 to 6, and the buoyancy influence parameter Ω ranging from -0.3 to 5.0, dimensionless values of the local heat transfer coefficient h_N, average heat transfer coefficient from an isothermal fin $\bar{h}_N$, local fin temperature θ_f, local heat flux q_N, overall fin heat transfer rate Q_N, fin effectiveness Φ based on an isothermal fin, local friction factor $C_f\mathrm{Re}^{1/2}$, and average friction factor $\bar{C}_f\mathrm{Re}^{1/2}$ were determined from the relations

$$\bar{h}_N=\int_0^1 h_N(X)\,dX$$

$$q_N=\left[\frac{qL}{K(T_0-T_\infty)}\right]\mathrm{Re}^{-1/2}=h_N\theta_f$$

Table 1 Average heat transfer coefficient for an isothermal fin $\bar{h}_N$ (Pr=0.7)

R_0	$\Omega=0$	$\Omega=1$	$\Omega=2$	$\Omega=5$	$\Omega=-0.3$
1	1.0650	1.1284	1.1732		
4/3	0.9562	1.0229	1.0688		
2	0.8474	0.9196	0.9677		
4	0.7258	0.8068	0.8580	0.9590	0.6779

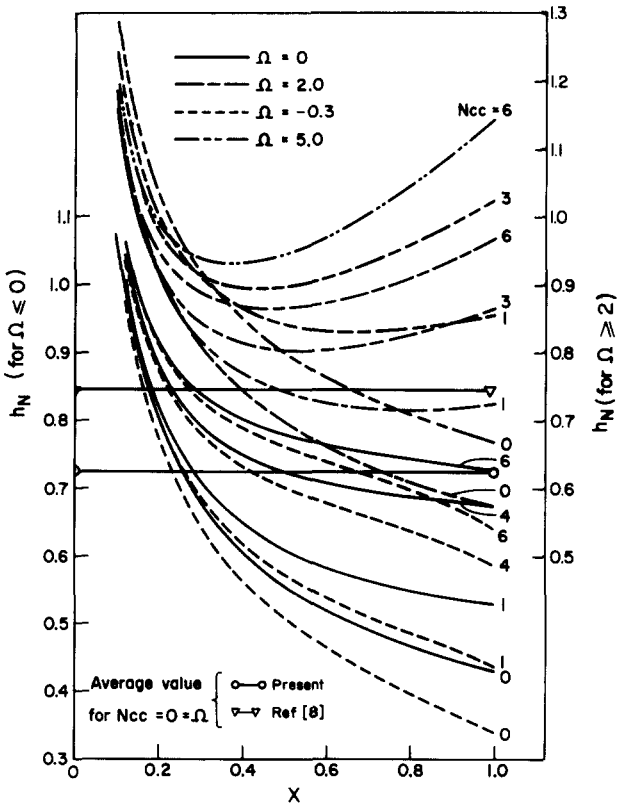

Figure 2 Local heat transfer coefficient (Pr=0.7, R_0=4)

$$Q_N=\left[\frac{Q}{r_0K(T_0-T_\infty)}\right]\mathrm{Re}^{-1/2}=\frac{2\pi}{N_{cc}}\frac{\mathrm{d}\theta_f(X=1)}{\mathrm{d}X}$$

$$\Phi=\frac{Q_N}{2\pi\bar{h}_N},\quad C_f=\frac{\tau}{\frac{1}{2}\rho u_\infty^2},\quad \bar{C}_f=\int_0^1 C_f\,\mathrm{d}X$$

where q and Q respectively are the dimensional counterparts of q_N and Q_N, τ is the shear stress on the fin surface, and ρ is the density of the fluid. The conduction equation for θ_f in the simple model yields[10]

$$\theta_f=\cosh(N_{cc}\bar{h}_N X^2)^{1/2}/\cosh(N_{cc}\bar{h}_N)^{1/2}$$

and the relations for q_N, Q_N, and Φ in the simple model are

$$q_N=\bar{h}_N\theta_f$$

$$Q_N=2\pi(\bar{h}_N/N_{cc})^{1/2}\tanh(N_{cc}\bar{h}_N)^{1/2}$$

and

$$\Phi=\tanh(N_{cc}\bar{h}_N)^{1/2}/(N_{cc}\bar{h}_N)^{1/2}$$

Heat transfer coefficient

The variation of the local heat transfer coefficient over a fin of radius $R_0=4$ is shown in Figure 2 for various values of Ω and N_{cc}. Observe that for $\Omega=0$, any N_{cc} value as well as for $N_{cc}=0$ and any Ω value, the local heat transfer coefficient decreases monotonically in the flow direction as the boundary layer grows. However, it increases (for the entire fin length) as N_{cc} increases for a fixed $\Omega\leqslant 0$, since a high value of N_{cc} means a high flow rate and a high conductivity of the fluid. For $\Omega>0$ and $N_{cc}>0$, the h_N-X curves display a minima whose location shifts toward the tip as N_{cc} increases. Also for $\Omega>0$, h_N decreases slightly with increasing N_{cc} near the tip. This can be explained as follows. As N_{cc} increases, the tip temperature decreases, rendering the effects of buoyancy less severe than that of fin surface friction. This dominating surface friction decelerates the fluid and reduces the heat transfer coefficient. The minima of these curves shift toward the tip because the higher the values of N_{cc} and Ω, the quicker the fluid picks up heat from the fin and the better the acceleration of the fluid, thereby causing the buoyancy to dominate over the surface friction and enhancing the heat transfer coefficient. Unlike the case where $\Omega>0$, the heat transfer coefficient in the case where $\Omega<0$ decreases along the flow, exhibiting a saddle point; the saddle point is more visible for higher N_{cc} values.

The local heat transfer coefficient for a fin of radius $R_0=\frac{4}{3}$ in forced convective flow is shown in Figure 3. It is clear from Figures 2 and 3 that the heat transfer coefficient increases as R_0 decreases. One reason for this is that the heat convection area decreases with decreasing fin radius. The other reason, more important than the former but not explained in Ref. 8, is that the heat flux that enters the fin from the base increases with decreasing fin radius. This point will be given further attention later. The average value of h_N for isothermal fins of various radii is presented in Table 1.

Local heat flux

The local heat flux along with the prediction of a simple model is presented in Figures 4 and 5. To avoid duplication, the heat flux for isothermal cases is not presented, since it is the same as the

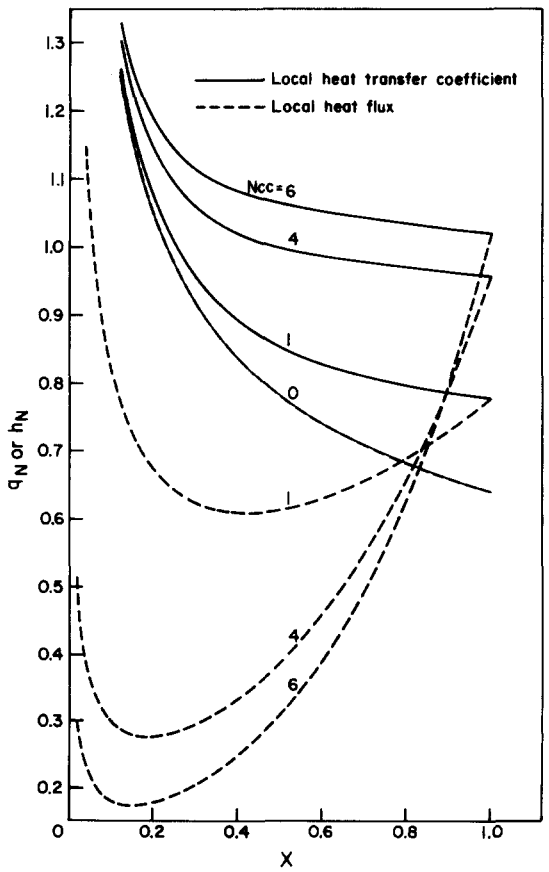

Figure 3 Local heat transfer coefficient and local heat flux for Pr=0.7, $R_0=\frac{4}{3}$, $\Omega=0$

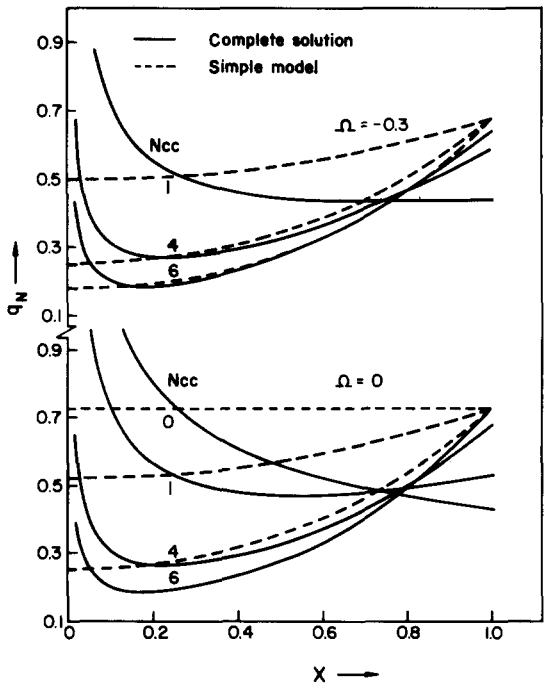

Figure 4 Local heat flux along the fin surface (Pr=0.7, R_0=4)

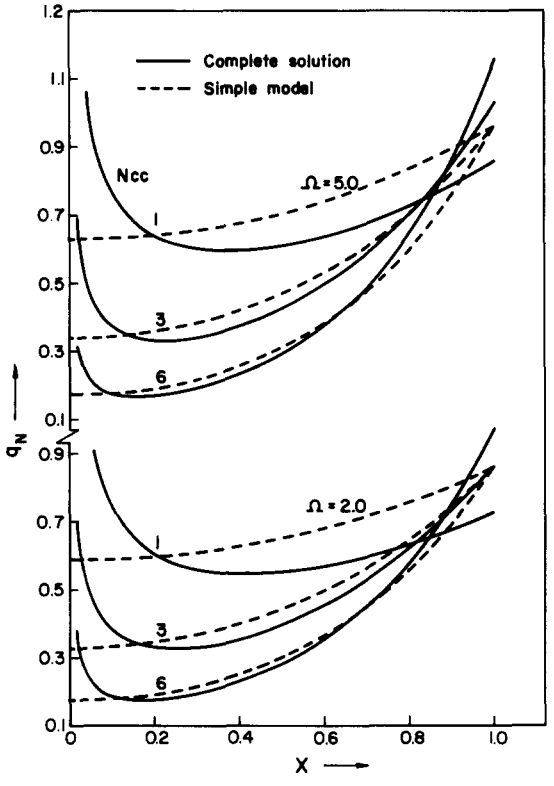

Figure 5 Local heat flux along the fin surface (Pr=0.7, R_0=4)

heat transfer coefficient given in Figure 2. From Figures 4 and 5 it is clear that the simple model underpredicts the heat flux in the region near the tip and overpredicts it in the rest of the region for low N_{cc} and all Ω values. As N_{cc} increases, the difference between the two models decreases for small Ω values. But as the effect of buoyancy increases for large N_{cc} values, the difference again increases, though only in the region near the base. In fact, the simple model underpredicts the heat flux near the base for large N_{cc} and Ω values. For a fixed value of N_{cc} the heat flux increases with Ω due to increased buoyancy effects.

It is also clear that the heat flux decreases as N_{cc} increases, since the fin temperature decreases with increasing N_{cc} except for a small region near the base of the fin. This holds for all Ω values. Another important observation from Figures 4 and 5 is that the areas under the corresponding heat flux curves of the simple and complete models are almost the same. This enables the simple model to predict the overall fin heat transfer rate with an amazing accuracy. From a comparison of Figures 3 and 4 it is clear that the heat flux increases with decreasing radius of the fin. This is because the heat flux that enters the fin from the base increases with decreasing radius, and the heat convective area decreases with the fin radius.

Fin temperature distribution

The fin temperature distribution predicted by both models is presented in Figure 6 for a fin of radius $R_0=4$. It is clear that the temperature predicted by the simple model (dashed lines) is always higher than the one that really prevails (solid lines) for all values of N_{cc} and Ω. However, as Ω increases, the difference between the two models decreases for all N_{cc} values. As N_{cc} increases, the temperature distribution becomes less uniform and the tip temperature decreases due to decreased fin conductance ($K_f r_0$) and/or increased convective effects.

Figure 7 shows the computed temperature distribution (solid lines) for a fin of radius $R_0=\frac{4}{3}$ in forced convective flow. A comparison of Figures 6 and 7 shows that for fixed values of N_{cc} and Ω the fin temperature becomes less uniform and the tip temperature decreases with decreasing radius of the fin as the fin conductance decreases. Figure 7 also compares the fin

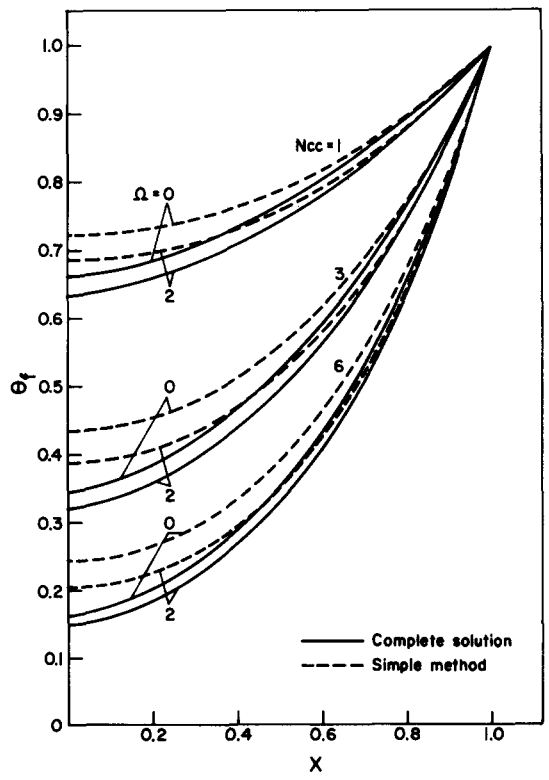

Figure 6 Fin temperature distributions (Pr=0.7, R_0=4)

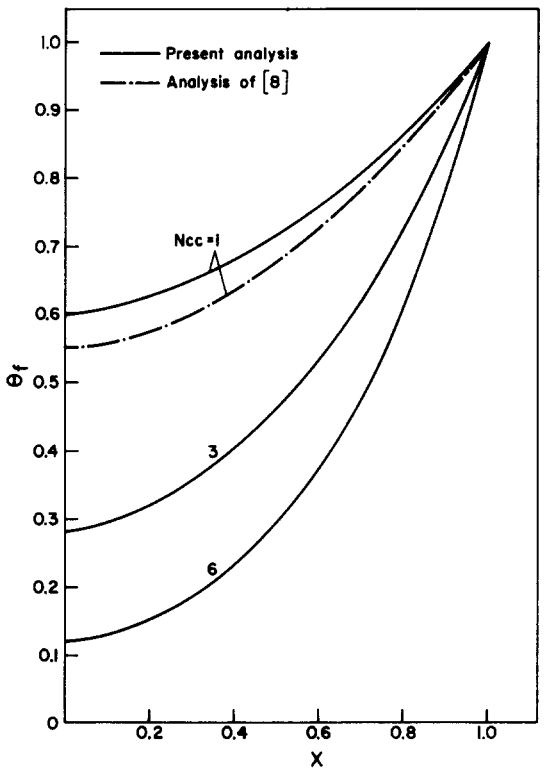

Figure 7 Fin temperature distributions (complete solutions); $\Omega=0$; $R_0=\frac{4}{3}$; Pr=0.7

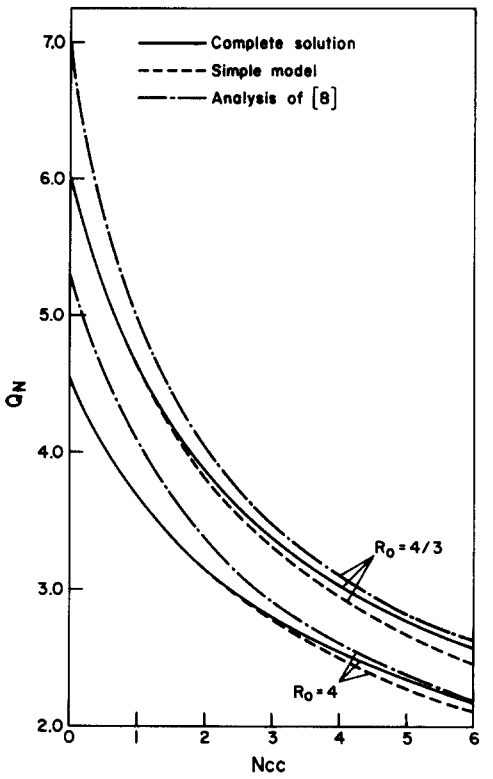

Figure 8 Overall fin heat transfer rate for Pr=0.7, $\Omega=0$

temperature distribution presented in Ref. 8 (chain line) with the present analysis. The analysis of Ref. 8 underpredicts the temperature distribution for both fin radii ($R_0=4$ and $\frac{4}{3}$) and both values of N_{cc} (1 and 4), though we present the comparison only for $R_0=\frac{4}{3}$ and $N_{cc}=1$. Deviations of at least 8.3% and 19% were observed for $N_{cc}=1$ and 4, respectively, for fin radii $R_0=4$ and $\frac{4}{3}$. Because of this underprediction of the fin temperature distribution, a temperature gradient steeper than the one that really prevails is expected at the base of the fin, thereby increasing the total heat transfer rate.

Fin temperature distribution for other cases can be obtained from corresponding heat transfer coefficients and the heat fluxes.

Overall heat transfer rate

The overall heat transfer rate (solid lines) for forced and mixed convective flows is presented in Figures 8–10 along with predictions of the simple model (dashed lines). As expected from the above results, the overall heat transfer rate decreases with increasing N_{cc} as the fin conductance decreases and the fin becomes more nonisothermal. For $\Omega\geqslant 0$, the simple model overpredicts (almost negligibly) the overall heat transfer rate at small N_{cc} values (except for $N_{cc}=0$) and underpredicts the same for high N_{cc} values. For $\Omega<0$, however, the simple model underpredicts the overall heat transfer rate for all values of N_{cc} except 0. The maximum difference between the two models at the largest N_{cc} value is 2.3% for $R_0=4$ and $\Omega=0$, and 3.9% for $R_0=\frac{4}{3}$ and $\Omega=0$. However, the difference decreases with increasing Ω-values. Also observe that the overall heat transfer rate increases when the buoyancy assists the main flow, and decreases when the same opposes the main flow.

Also shown in Figure 8 is the overall heat transfer rate of

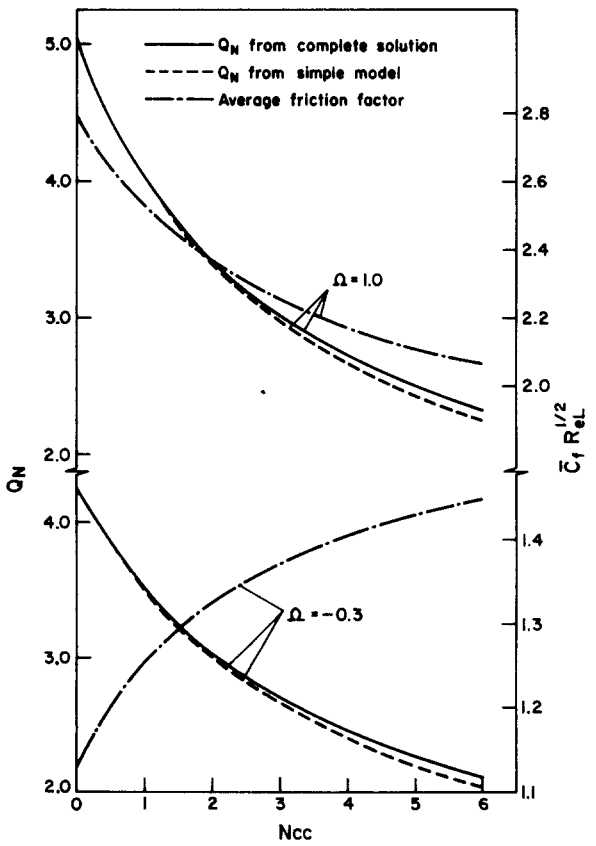

Figure 9 Overall fin heat transfer rate and average shear stress for Pr=0.7, $R_0=4$

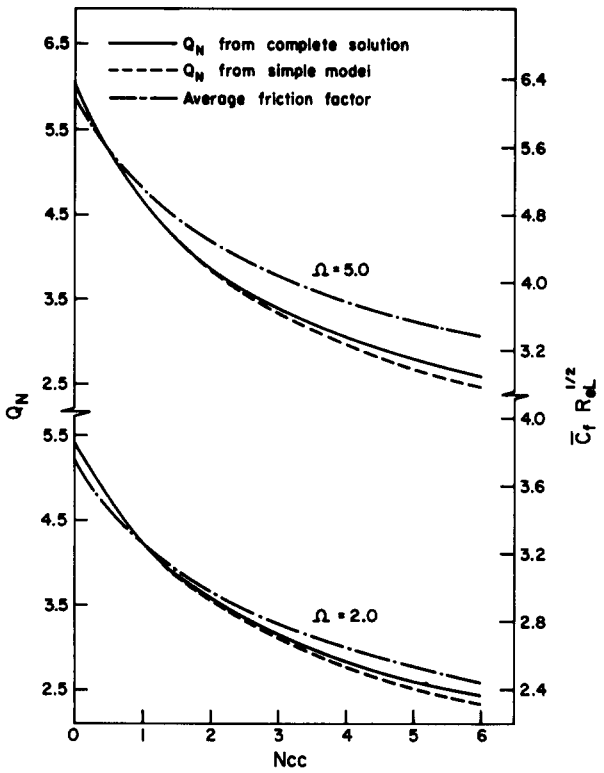

Figure 10 Overall fin heat transfer rate and average shear stress for Pr=0.7, R_0=4

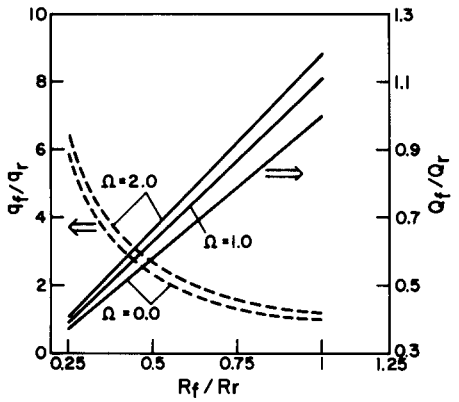

Figure 11 Effect of fin radius (N_{cc}=0, Pr=0.7)

Huang and Chen[8]. Their analysis overpredicts the heat transfer rate even for $R_0=4$ and $N_{cc}=0$, for which the local values of heat transfer coefficient and heat flux matched with our results exactly. Figure 1 of Ref. 8 predicts $\bar{h}_N=0.847$ for $R_0=4$, $N_{cc}=0$, $\Omega=0$, whereas the actual value is $\bar{h}_N=0.726$, as shown in Figure 2.

Figure 11 depicts the effect of fin radius on the total heat transfer rate and the heat flux that enters into the fin from the base. The reference fin, for the results presented in Figure 11, is taken as the fin of radius R_r ($=R_0$)=4 in forced convective flow ($\Omega=0$). The left ordinate represents the ratio of heat flux for this reference fin to that for the fin of radius R_f. The right ordinate represents a similar ratio for the total heat transfer rate. It is clear that the total heat transfer rate (solid lines) increases with R_f and Ω. The heat flux that enters the fin at the base increases with decreasing radius of the fin and increasing buoyancy effects (dashed lines). This explains why many smaller-diameter fins can transfer more heat than a smaller number of larger-diameter fins.

Fin effectiveness

The fin effectiveness Φ (for the complete model) based on the corresponding isothermal fin is presented in Figure 12. The fin effectiveness decreases as either Ω or N_{cc} increases, since the fin temperature distribution becomes less uniform when either Ω or N_{cc} increases. We also mention, without displaying such results, that fin effectiveness increases with fin radius, owing to increasing uniformity in the fin temperature distribution. Fin effectiveness for the simple model can be obtained from Figures 8–10 and the relation $\Phi=Q_N/2\pi\bar{h}_N$. Table 2 shows that for $\Omega\geq 0$ the simple model overpredicts the effectiveness at small N_{cc} values and underpredicts the same at large N_{cc} values, but for $\Omega<0$ it always underpredicts the effectiveness. This result is also in accord with the analysis of rectangular fins[3].

Friction factor

The local and average friction factors have been presented in Figures 13, 9, and 10. For $\Omega>0$ the local friction factor displays a minima for all N_{cc} values. The negative slope of the curves indicates the deceleration of the fluid by the effect of surface friction, and the positive slope of the curves indicates the acceleration of the fluid by the effect of buoyancy. For a fixed value of $\Omega>0$ the local friction factor decreases with increase in

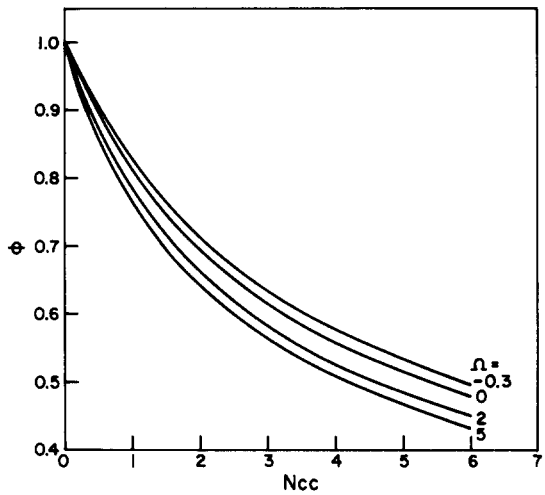

Figure 12 Fin effectiveness based on an isothermal fin for Pr=0.7, R_0=4 (complete solution)

Table 2 Fin effectiveness Φ (R_0=4; Pr=0.7)

	Ω=−0.3		Ω=0		Ω=2	
N_{cc}	Simple model	Complete solution	Simple model	Complete solution	Simple model	Complete solution
1	0.822	0.826	0.812	0.812	0.787	0.785
3	0.625	0.634	0.610	0.615	0.575	0.583
6	0.479	0.497	0.465	0.48	0.431	0.45

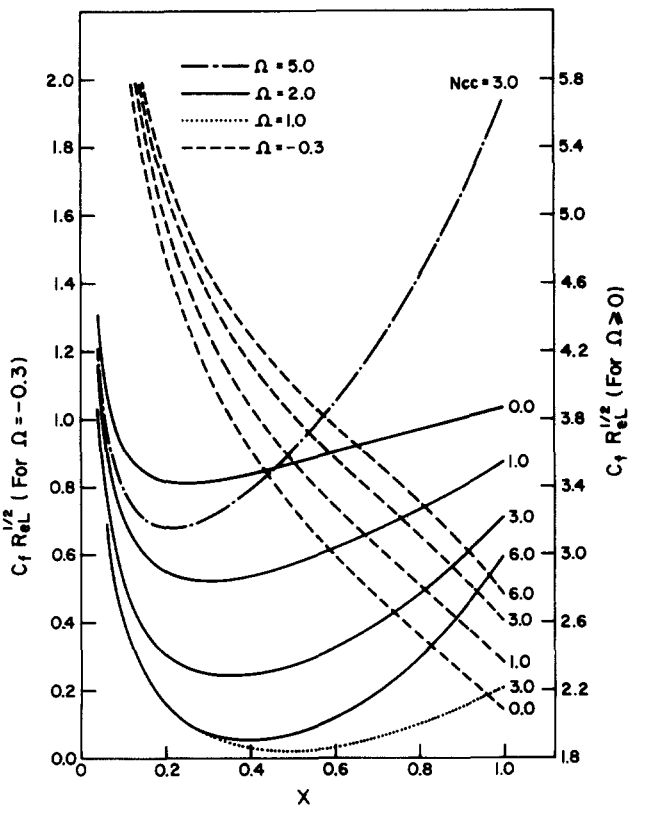

Figure 13 Local friction factor for Pr=0.7, R_0=4

N_{cc}, thereby decreasing the average friction factor as well. The friction factor approaches the value for forced convection as $N_{cc} \to \infty$ ($N_{cc} \to \infty$ implies a completely insulated fin). For a fixed value of N_{cc} the local and average friction factors increase with Ω, due to increased buoyancy effects.

For $\Omega < 0$ the local and, hence, the average friction factors increase with N_{cc}. The local friction factor curves for $\Omega < 0$ approach the zero value—the sign for flow reversal. The chance for flow reversal is maximum for the isothermal case, and it decreases as N_{cc} increases.

Conclusions

The problem of laminar, conjugate forced and mixed convective flows (both when the buoyancy assists and when it opposes the main flow) over a cylindrical fin has been studied. A very simple and efficient numerical method has been devised for the solution. The effects of various parameters, such as the buoyancy influence parameter Gr/Re^2, dimensionless radius of the fin R_0, and the conduction convection parameter $(2KL/K_f r_0)Re^{1/2}$ on the heat transfer characteristics, have been studied. Results of the complete numerical solution have been presented along with the results of the simple model. The simple model produces satisfactory results for the overall heat transfer rate, but the local predictions are in substantial error. Results are important for accurate heat transfer calculations from fins.

Acknowledgments

The computing facility made available at the Indira Gandhi Centre for Atomic Research, Kalpakkam, India is gratefully acknowledged. The second author would also like to acknowledge the support from The Ohio State University during the sabbatical.

References

1 Sparrow, E. M. and Chyu, M. K. Conjugate forced convection-conduction analysis of heat transfer in a plate fin. *ASME J. Heat Transfer* 1982, **104**, 204–206

2 Sparrow, E. M. and Acharya, S. A natural convection fin with a solution-determined nonmonotonically varying heat transfer coefficient. *ASME J. Heat Transfer* 1981, **103**, 218–225

3 Sunden, B. Conjugate mixed convection heat transfer from a vertical rectangular fin. *Int. Comm. Heat Mass Transfer* 1983, **10**, 267–276

4 Sunden, B. A numerical investigation of coupled conduction-mixed convection for rectangular fins. Proc. 3rd Int. Conf. Numerical Methods in Laminar and Turbulent Flow, Pineridge Press, 1983, pp. 809–819

5 Garg, V. K. and Velusamy, K. Heat transfer characteristics for a plate fin. *ASME J. Heat Transfer* 1986, **108**, 224–226

6 Sunden, B. The effect of Prandtl number on conjugate heat transfer from rectangular fins. *Int. Comm. Heat Mass Transfer* 1985, **12**, 225–232

7 Cebeci, T. and Bradshaw, P. *Momentum Transfer in Boundary Layers*. Hemisphere, Washington, D.C., 1977

8 Huang, M. J. and Chen, C. K. Vertical circular pin with conjugated forced convection-conduction flow. *ASME J. Heat Transfer* 1984, **106**, 658–661

9 Huang, M. J., Chen, C. K., and Cleaver, J. W. Vertical circular pin with conjugated natural convection-conduction flow. *ASME J. Heat Transfer* 1985, **107**, 242–245

10 Eckert, E. R. G. and Drake, R. M. *Analysis of Heat and Mass Transfer*. McGraw-Hill, Tokyo, 1972

11 Hornbeck, R. W. *Numerical Marching Techniques for Fluid Flows with Heat Transfer*. NASA SP-297, Washington, D.C., 1973

12 Yu, H. S. and Sparrow, E. M. Local nonsimilarity thermal boundary layer solutions. *ASME J. Heat Transfer* 1971, **93**, 328–334

13 Chen, T. S. and Mucoglu, A. Buoyancy effects on forced convection along a vertical cylinder. *ASME J. Heat Transfer* 1975, **97**, 198–203